INTERNATIONAL JOURNAL FOR NUMERICAL METHODS IN FLUIDS
Int. J. Numer. Meth. Fluids 2007; **54**:945–963
Published online 17 April 2007 in Wiley InterScience (www.interscience.wiley.com). DOI: 10.1002/fld.1474

A framework for stabilized partitioned analysis of thin membrane–wind interaction

Roland Wüchner*,†, Alexander Kupzok and Kai-Uwe Bletzinger

Lehrstuhl für Statik/Chair of Structural Analysis, Technische Universität München, Arcisstr. 21, München D-80290, Germany

SUMMARY

This contribution proposes a methodology for the numerical analysis and for the improvement of the design of free-form membrane structures subjected to flow-induced effects. Typical applications in such context are tents exposed to wind. Different physical factors connected to thin and flexible structures, highly turbulent air flows, as well as their interaction have to be taken into account. This necessitates the appropriate combination of different numerical disciplines which is done in the simulation of fluid–structure interaction. The over-all complexity of the problem favours a modular and flexible software environment with a partitioned coupling strategy. Within such an environment, the solution of each physical and algorithmic field is applicable with the most suited method. In the proposed framework, the structural field is solved with the in-house finite element program CARAT, which uses several finite element types and advanced solution strategies for form finding, nonlinear, and dynamical problems. The fluid field is solved with the CFD software package CFX-5. The interaction between both physical fields is realized by the exchange of boundary conditions. Beyond the mere exchange of data, the utilization of stabilized as well as efficient coupling strategies is mandatory. This contribution illuminates the scope of numerical simulation theory and presents implementations followed by illustrative examples. Copyright © 2007 John Wiley & Sons, Ltd.

Received 15 December 2006; Revised 5 February 2007; Accepted 6 February 2007

KEY WORDS: fluid–structure interaction; free-form shape; stabilized partitioned analysis; coupling algorithms; aeroelasticity

*Correspondence to: Roland Wüchner, Lehrstuhl für Statik, Technische Universität München, Arcisstr. 21, München D-80290, Germany.
†E-mail: wuechner@bv.tum.de

1. INTRODUCTION

1.1. Motivation

Membranes are extremely light and slender constructions because of the optimal use of material by a constant stress state over the thickness. Typically, the resulting shape is a free-form membrane which cannot be described analytically [1]. In the case of structures subjected to loads from a surrounding fluid, increasing lightness and slenderness causes a higher susceptibility to flow-induced deformations and vibrations. Examples of applications from civil engineering are wind effects on thin shell and membrane structures.

Wind effects can define decisive design loads and therefore require in-depth analysis. Such an analysis is very challenging in the cases of interaction between structure and wind [2]. In civil engineering, these interactions occur on constructions such as towers, high-rise buildings, bridges, cable and membrane roofs, etc.

The standard procedure in structural engineering is to reduce the complex problem of structures subjected to wind to simpler models by finding appropriate assumptions. However, this approach involves the risk of neglecting effects which result from the strong coupling of the two different physical fields. Regarding light-weight structures, the analysis of interdependencies between structure and wind is of great importance.

For such an analysis, the application of numerical simulations for aeroelastic effects is a promising complement to and enhancement of experimental approaches. The simulation of phenomena of aeroelasticity necessitates the appropriate combination of different numerical disciplines which is done with a fluid–structure interaction (FSI) method [3].

1.2. Approach

The development of methods for FSI computations with light structures is a topic of ongoing research. Generally, two different types of approaches for the numerical simulation of FSI exist: monolithic [4–8] and partitioned strategies [9–13].

In the special case of light-weight structures subjected to wind, the following requirements are identified:

- Adequate solution of highly turbulent flows and modelling of fluid boundary conditions to represent the characteristics of physical wind.
- Treatment of moving boundaries in the fluid solver.
- Correct treatment of geometric nonlinearities in stationary and transient structural analysis.
- Integration of form finding to determine the proper initial geometry in the case of membrane structures due to strong coherence between shape and load carrying behaviour.
- Accurate transfer of coupling quantities, especially in the case of non-matching grids.
- Respect of strong coherences between the physical fields by stabilized coupling schemes.

Different FSI strategies are suited to address these requirements. The authors choose a partitioned approach as the most convenient for this problem type [13]. The choice is motivated by the possibility to solve all involved physical fields by specialized, adapted, and tested single-field solvers. The need for elaborate revising of existing codes towards multiphysics is evaded. The realization of physical coupling is handled with the exchange of boundary conditions [14–17] using stabilized and efficient coupling strategies. In the current approach, the form finding and structural analysis parts are solved utilizing the research code CARAT. The fluid part is solved

DOI: 10.1002/fld

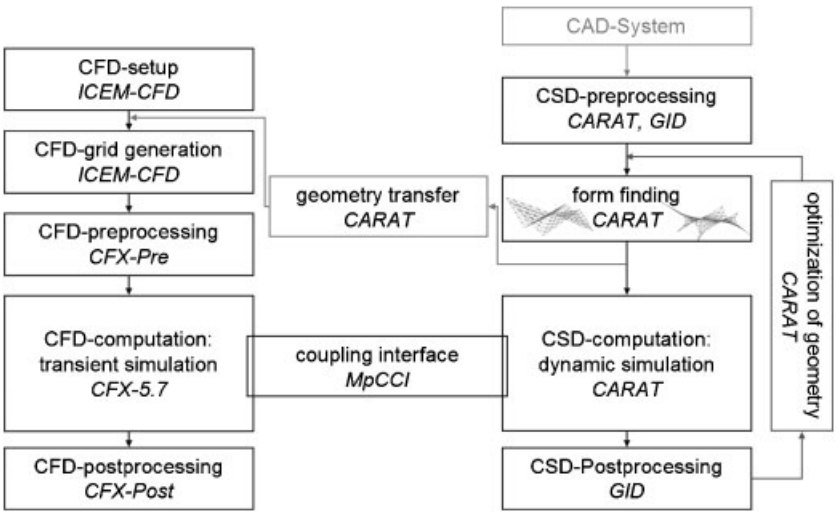

Figure 1. Software environment and workflow of a coupled simulation.

by the general purpose computational fluid dynamics code CFX-5 of Ansys Inc. [18]. For the exchange of boundary conditions, the library MpCCI [19] is used.

Figure 1 provides a detailed view of the software environment and procedure of a coupled simulation.

2. FLUID PART

The viscous fluid flow is described by the governing Navier–Stokes equations which state the conservation of mass (Equation (1)) and momentum (Equation (2)):

$$\frac{\partial \rho}{\partial t} + \frac{\partial}{\partial x_i}(\rho U_i) = 0 \tag{1}$$

$$\frac{\partial}{\partial t}(\rho U_j) + \frac{\partial}{\partial x_i}(\rho U_i U_j) = -\frac{\partial P}{\partial x_j} + \frac{\partial}{\partial x_i}\left(\mu_{\text{eff}}\left(\frac{\partial U_j}{\partial x_i} + \frac{\partial U_i}{\partial x_j}\right)\right) \tag{2}$$

with U_j as the velocity component in the j-direction, x_i as the Cartesian coordinate in the i-direction, P as the pressure, $\mu_{\text{eff}} = \mu + \mu_{\text{t}}$ as the effective viscosity, consisting of the dynamic viscosity μ and the turbulent viscosity μ_{t}. ρ represents the density of the fluid.

In the scope of this work, the finite volume approach is used to solve the Navier–Stokes equations for incompressible fluids. Equations of mass conservation and momentum conservation are applied to control volumes whose boundaries move with time. Equations (1) and (2) can be expressed in integral form and by considering the grid velocity $U_{g,i}$ and the incompressible fluid state simplified to Equations (3) and (4). This is known as the arbitrary Lagrangian Eulerian (ALE)

DOI: 10.1002/fld

formulation [20]:

$$\int_S \rho U_{g,i}\,\mathrm{d}S_i - \int_S \rho U_i\,\mathrm{d}S_i = 0 \tag{3}$$

$$\rho\frac{\mathrm{d}}{\mathrm{d}t}\int_V U_j\,\mathrm{d}V - \rho\int_S \left(U_{g,i} - U_i\right)U_j\,\mathrm{d}S_i = -\int_S P\,\mathrm{d}S_i + \int_S \mu_{\mathrm{eff}}\frac{\partial U_j}{\partial x_i}\,\mathrm{d}S_i \tag{4}$$

In the sequel, the transient term in Equation (4) is approximated as

$$\rho\frac{\mathrm{d}}{\mathrm{d}t}\int_V \Phi\,\mathrm{d}V = \rho V\frac{\Phi(t_{n+1}) - 4\Phi(t_n) + \Phi(t_{n-1})}{2\Delta t} \tag{5}$$

where $\Delta t = t_{n+1} - t_n$ is the time step size and $\Phi(t_n)$ ($\Phi(t_{n-1})$) represents the solution field at the previous time step t_n (the time step before the previous time step t_{n-1}). This specifies a second-order backward-Euler scheme which requires an iterative solution method, is implicit and therefore, does not create any time step limitation.

In the present work, CFD calculations are performed by the commercial computational fluid dynamics package CFX-5 [18]. CFX-5 solves the 3D Navier–Stokes equations on structured and unstructured grids for compressible and incompressible flows. For the simulation of turbulent flows several advanced turbulence models are available, including Reynolds-averaged Navier–Stokes models (RANS), large Eddy simulations (LES), and detached Eddy simulations (DES). For the following examples, the shear-stress-transport (SST) model was applied [21]. An advanced multigrid solver capable of parallelization is applied for efficient computing.

By applying the above-mentioned ALE approach, CFX-5 offers the possibility of moving and deforming grids such as they are necessary for the deformation of a FSI interface during a coupled simulation [18, 22]. The adaptation of the CFD grid to the updated boundary conditions is performed by solving a diffusion problem. This resembles a special case of the mesh moving model proposed in the papers [23, 24]:

$$\begin{gathered}\nabla(K_{\mathrm{Mesh}}\nabla x) = 0\\ \text{with } x|_{\Gamma_b} = x_b \text{ for deformed surfaces}\\ \text{and } x|_{\Gamma_0} = 0 \text{ for undeformed surfaces}\end{gathered} \tag{6}$$

with x as the displacement of the CFD mesh, K_{Mesh} as the mesh stiffness and ∇ as the gradient operator. In order to prevent self-penetration of the finite volume elements in the adapted CFD computation grid, it has been proved useful to increase the 'Mesh Stiffness' of especially small finite volume cells by setting parameter K_{Mesh} to:

$$K_{\mathrm{Mesh}} = \left(\frac{1}{V_{\mathrm{FVE}}}\right)^m \tag{7}$$

where V_{FVE} is the volume of a specific finite volume cell and m a natural number. For numbers $m>3$, depending on the volume of the smallest finite volume cell and the computational precision, floating point exceptions are likely to occur. However, increasing the 'mesh stiffness' depending on the volume of the finite volume cells does not diminish the susceptibility of the finite volume cells towards distortion.

DOI: 10.1002/fld

3. STRUCTURE PART

The structural problem is characterized by the governing equations for an elastic body with large deformations (and the corresponding boundary and initial conditions): dynamic equilibrium (8), kinematics (9), and material law (10). If only stationary problems are considered, the acceleration vector $\ddot{\mathbf{d}}$ disappears and Equation (8) reduces to the static equilibrium condition. Cauchy's first equation of motion in local form for each point $\mathbf{X}$ of the reference configuration Ω_{S0} and all times t states as

$$\rho_{S0}\ddot{\mathbf{d}} = \nabla \cdot (\mathbf{FS}) + \rho_{S0}\mathbf{B} \tag{8}$$

where ρ_{S0} is the density in the undeformed configuration, $\mathbf{F}$ the deformation gradient, $\mathbf{S}$ the second Piola–Kirchhoff stress tensor (PK2) and $\mathbf{B}$ the reference body force. The Green–Lagrange strain tensor is computed by

$$\mathbf{E} = \tfrac{1}{2}(\mathbf{F}^{\mathrm{T}}\mathbf{F} - \mathbf{I}) \tag{9}$$

and the linear relation between stress and strain is defined with the help of the elasticity tensor $\mathbf{C}$

$$\mathbf{S} = \mathbf{C} : \mathbf{E}, \quad \mathbf{C} = \lambda \mathbf{I} \otimes \mathbf{I} + 2\mu \mathscr{I} \tag{10}$$

which represents the St. Venant–Kirchhoff material law for isotropic materials which is used within this contribution. The elastic material behaviour of isotropic solids is fully described by two material constants: either in terms of Young's modulus E and Poisson's ratio ν or the Lamé constants λ and μ:

$$\lambda = \frac{\nu E}{(1+\nu)(1-2\nu)}, \quad \mu = G = \frac{E}{2(1+\nu)} \tag{11}$$

This results in the following stress–strain relation:

$$\mathbf{S} = \lambda \operatorname{tr}(\mathbf{E})\,\mathbf{I} + 2\mu\mathbf{E} \tag{12}$$

The geometry of the membrane is described by two surface parameters θ^1 and θ^2 and quantities in the undeformed configuration are designated by upper-case and in the deformed configurations by lower-case letters, respectively. The curvilinear base vectors are defined by

$$\mathbf{g}_\alpha = \mathbf{x}_{,\alpha} = \frac{\partial \mathbf{x}}{\partial \theta^\alpha} \quad \text{as well as} \quad \mathbf{G}_\alpha = \mathbf{X}_{,\alpha} = \frac{\partial \mathbf{X}}{\partial \theta^\alpha} \tag{13}$$

The deformation of a point of the membrane surface depends on the difference of its locations in space:

$$\mathbf{d}(\theta^1, \theta^2, t) = \mathbf{x}(\theta^1, \theta^2, t) - \mathbf{X}(\theta^1, \theta^2) \tag{14}$$

These governing equations of the membrane dynamics are solved by the finite element method. For this purpose, the Lagrangian description is used, i.e. the nodes of the corresponding mesh are fixed to the material points. By using the isoparametric approach, the nodal positions ($\bar{\mathbf{X}}_i$ and $\bar{\mathbf{x}}_i$) and the three displacements ($\bar{\mathbf{d}}_i$) per node are interpolated by the same shape functions. This leads to the semi-discrete equations of motion

$$\mathbf{M}\ddot{\bar{\mathbf{d}}}_\alpha [+\mathbf{D}\dot{\bar{\mathbf{d}}}_\alpha] + \mathbf{r}_{\mathrm{int}}(\bar{\mathbf{d}}_\alpha) = \mathbf{r}_{\mathrm{ext}\,\alpha}(t) \tag{15}$$

DOI: 10.1002/fld

where $\mathbf{M}$ is the mass matrix, $\mathbf{D}$ the damping matrix representing the structural damping (if considered in the simulation), $\mathbf{r}_{\text{int}}$ the vector of internal forces which leads *via* linearization to the tangential stiffness matrix and $\mathbf{r}_{\text{ext}}$ the vector of external loads (which are assumed to be deformation-independent) acting on the structure.

This nonlinear time-dependent problem with properly defined boundary and initial conditions is solved by a time integration algorithm. In the presented example, the (implicit) generalized-α method [25] was used because of its advantageous properties: with a certain choice of parameters, the procedure is second-order accurate and the user has full control of the numerical dissipation of the spurious high frequencies by minimizing errors in the lower modes of interest.

In the proposed partitioned approach the fluid–structure coupling only affects the right-hand side of (15) neglecting the obvious displacement dependence of the fluid load which would lead to additional contributions during linearization [26]. This is due to the fact that the classic follower-force formulation would not be able to adequately represent the physical processes in the fluid field. Hence, the interaction of the physical fields is realized by appropriate coupling algorithms.

The structures under consideration are described by membrane theory, which is based on the assumption that the bending and transverse shear effects disappear. Furthermore, the negligibly small thickness h is assumed to be constant during deformation. The latter has an important impact on the formulation of the coupling interface, i.e. the fluid solver must be able to deal with infinitely thin bodies.

Due to the inherent coupling of stress state and membrane shape, the geometry of the undeformed, but already stressed, structure must be determined in a separate analysis. This is, naturally, the first step for a computation concerning membrane structures (see Figure 1). The initial shape for the analysis of a membrane interacting with a surrounding fluid is defined by the equilibrium of surface stresses and edge cable forces, found as the result of a form finding computation [27]. The need for special form finding procedures results from the singularity of the inverse problem of finding the corresponding shape to a given stress distribution. This difficulty is overcome by the updated reference strategy [28], a regularization by a homotopy mapping which is implemented in CARAT.

After the initial shape is found, further analysis respecting wind or snow loads can be performed. For the coupled computation, naturally, this initial shape defines the FSI interface. However, if a certain shape exhibits problematic behaviour under wind action the pre-stress distribution must be modified so that the improved shape prevents flutter. This gives the perspective of a sequential application of form finding and FSI computation to find an ideal initial shape, which is least susceptible to wind, and the according pre-stress distribution. Such a sequential analysis can be realized by using the software environment proposed in this paper.

4. FLUID–STRUCTURE COUPLING

4.1. Coupling schemes for partitioned FSI analysis

Several different strategies can be used to solve FSI problems. In a so-called monolithical approach, all physical fields are solved in one single numerical model. Due to the complexity of the numerical simulation which is necessary to address the problems of interest, here a partitioned solution scheme is chosen. In a partitioned FSI simulation, the fluid and the structure simulation work together in a staggered algorithm. They exchange deformations and stresses as respective boundary conditions

DOI: 10.1002/fld

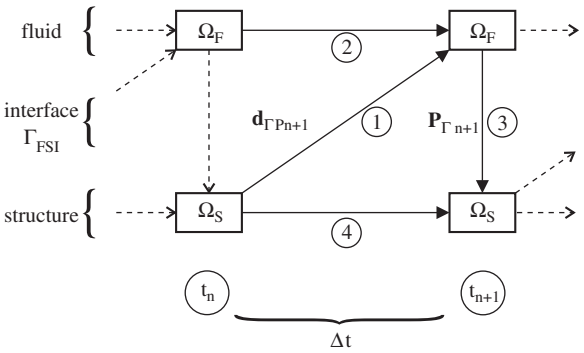

Figure 2. Explicit coupling scheme.

on the common interface. Here, the interface is the surface of the structure wetted by the fluid. The exchange of the boundary conditions has to fulfill requirements for the kinematic and dynamic continuity at the coupling interface [29, 30]. The main advantage of the approach is the fact that specialized and well-tested simulation codes for each physical field can be brought together to solve the coupled problem.

Stationary and time-dependent (transient) simulations are possible, whereas the first can be seen as a special case of the latter, only involving one time step. Depending on the physical problem and the computational resources, different coupling schemes are used. They result in different stabilities and accuracies of the solution of the coupled problem.

With a simple once-per-time step exchange of coupling quantities, a sequentially staggered or explicit coupling scheme is realized (see Figure 2). This explicit coupling scheme is very cheap with respect to computational costs, as there is only one necessary solution of the structural and the fluid field within one time step. However, inherent to this coupling scheme is a violation of interface conditions, since one physical field has only information about the other field at the beginning of the time step. Therefore, the kinematic continuity is, in general, not fulfiled because when computing the fluid field in time step t_{n+1}, the fluid solver has only information about the boundary condition (the geometry of the FSI interface) at the end of the previous time step t_n, which generally does not correspond to the interface geometry at the end of the time step t_{n+1}. To reduce this discrepancy in displacements, the kinematic coupling conditions can be extrapolated by a predictor $\mathbf{d}_{\Gamma P\, n+1}$ [29, 30].

As a consequence of the violation of the interface condition, the sequentially staggered algorithm shows weak instabilities whose occurrence cannot be prevented by simply reducing the time step size [31]. Especially in the case of FSI between incompressible flows and very light and flexible structures, the 'artificial added mass effect' deteriorates the stability properties of the coupling procedure dramatically [32]. This fictitious part of the added mass results from the violated kinematic continuity and acts instantaneously as an erroneous load on the structure. The described effect is even more pronounced, if the structural mass is very low, which proves the importance to control this phenomenon in the intended applications [15, 33, 34]. Foerster and Wall [35] identify a criterion to assess the stability of an explicit coupled simulation based on the ratio of the fluid density to the structural density.

To ensure an algorithmically strong coupling, an iterative staggered or implicit coupling scheme is realized through an additional inter-field iteration loop: several coupled computations are

DOI: 10.1002/fld

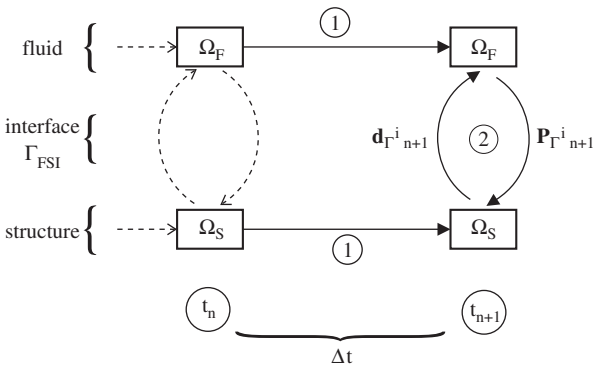

Figure 3. Implicit coupling scheme.

conducted until the coupling conditions are fulfiled within one time step and the next time level is entered (see Figure 3). Using the implicit coupling scheme, solutions of the partitioned method converge to solutions which are computed with a monolithical approach [36]. A downside of this approach is the fact that implicit treatment of the coupling conditions requires highly increased numerical effort. Therefore, additional attempts should be made to formulate efficient coupling strategies.

However, even implicit coupling schemes are not unconditionally stable for FSI problems with high structural deformations [31, 32]. In order to stabilize the coupled computation, under-relaxation of coupling quantities is used:

$$\mathbf{V}_{i+1} = \mathbf{V}_i + r_{i+1} \cdot \Delta\mathbf{V}_{i+1} \quad \text{with } \Delta\mathbf{V}_{i+1} = \tilde{\mathbf{V}}_{i+1} - \mathbf{V}_i \tag{16}$$

where $\mathbf{V}$ is a variable the under-relaxation is applied to, $\tilde{\mathbf{V}}$ is the non-under-relaxed variable, r is the under-relaxation factor, and i is the number of the inter-field iteration step within one time step. The under-relaxation technique can be applied on both boundary conditions which are exchanged between the two simulation codes, the surface load and the displacements.

Small under-relaxation factors provide a good behaviour of the coupled simulation towards stability for the price of a significantly higher computational effort, as more inter-field iterations are necessary to reach a dynamic equilibrium within a time step. Therefore, a reasonable choice for the parameter r is required as a compromise between numerical stability and efficiency. The specification of the optimal value for the relaxation parameter is a non-trivial task due to the nonlinearity of the problem and the strong dependency on the specific task. It is highly desirable to determine the proper value independent of any user input and according to the current system properties. Following the work of Mok and Wall [32], in this approach, the Aitken method for vector equations (as proposed in [37]) is applied. It introduces only minor (and therefore negligible) additional computational effort and provides a newly adapted value for the relaxation in each inter-field iteration step:

$$\mu_{i+1} = \mu_i + (\mu_i - 1)\frac{(\Delta\mathbf{V}_i - \Delta\mathbf{V}_{i+1})^{\mathrm{T}} \cdot \Delta\mathbf{V}_{i+1}}{|\Delta\mathbf{V}_i - \Delta\mathbf{V}_{i+1}|^2} \tag{17}$$

$$r_{i+1} = 1 - \mu_{i+1} \quad \text{with } \mu_1 = 0 \tag{18}$$

DOI: 10.1002/fld

4.2. Realization with the proposed environment

Based on the necessity of an implicit coupling scheme for the problems of interest, this chapter presents the discussion of the realization within the chosen software environment. The implementation of functionalities in the structural in-house FE-code CARAT are straightforward [38]. Therefore, here, the interface treatment and the necessary modifications of the fluid code are emphasized.

4.2.1. Discretization of the FSI interface. The main benefit of using MpCCI [19] is its ability to support different discretizations of the common interface. The possibility to transfer and interpolate mesh-based quantities between non-matching grids on the coupling interface of the structure and the fluid part ensures that each simulation code can work on an optimal mesh for the specific numerical simulation method.

For an interface concerning a membrane structure, the thickness of the structure is neglected and, accordingly, the structure is treated as an infinitesimally thin plane in both the fluid and the structural computation. In the fluid simulation this infinite thin structure possesses two interface surfaces, one on each side.

4.2.2. CFX. In this approach, CFX 5.7 of Ansys Inc., a commercial CFD package, is used to solve the fluid field [18]. When work is carried out with a commercial code like CFX, certain restrictions due to customization of the solution algorithm have to be taken into account.

In order to realize a coupling approach which satisfies the necessities identified in the previous subsection, the coupling algorithm between the fluid and the structural sides is realized as presented in Figure 4: the fluid and the structural simulation work together in a staggered algorithm, explicit and implicit coupling schemes are possible.

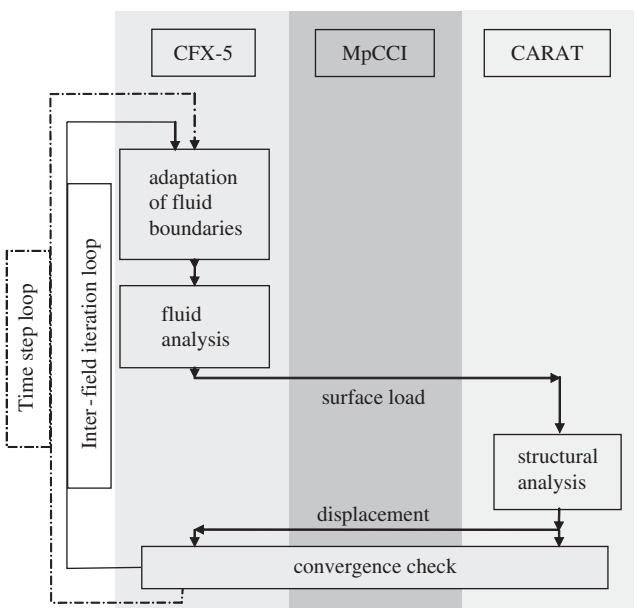

Figure 4. Flow chart of the coupling algorithm.

DOI: 10.1002/fld

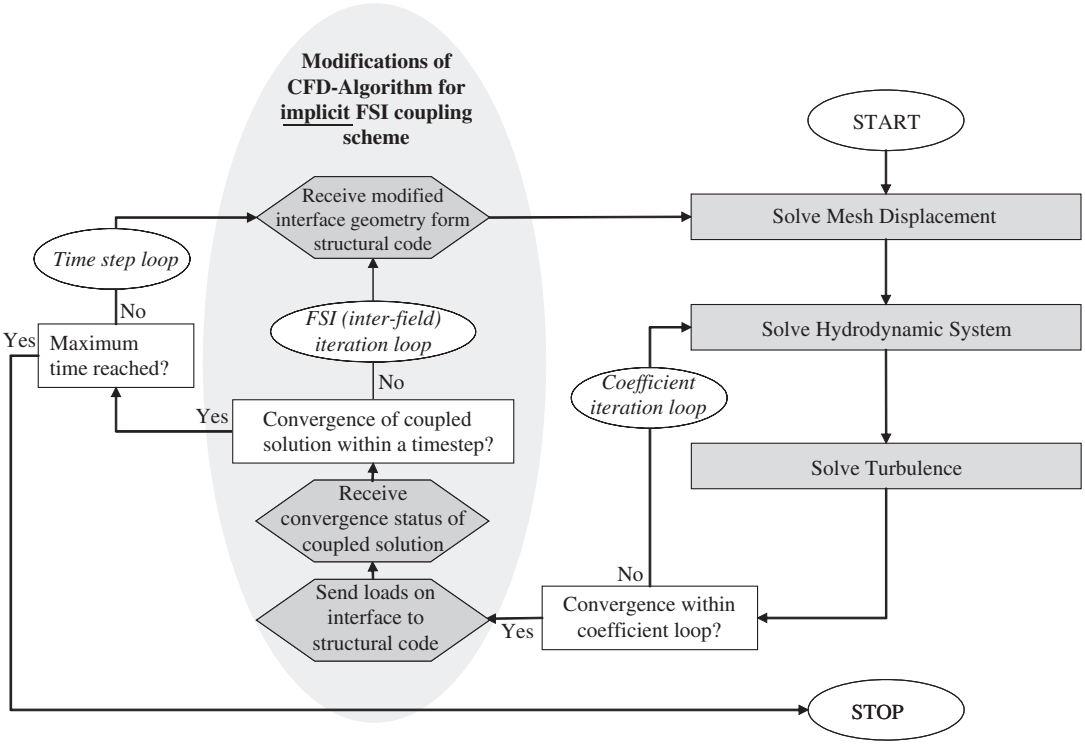

Figure 5. Extension of the CFX solution scheme for implicit FSI coupling.

Two main loops can be identified: the implicit inter-field iteration loop and the time step loop. The inter-field iteration loop is necessary to realize the implicit coupling scheme. This loop realizes an inter-field iteration by multiple exchanges of the boundary conditions on the interface which leads to a dynamic equilibrium of the coupled solution within one time step. After equilibrium within a time step is reached, the algorithm proceeds within the time step loop. Explicit coupling is realized by ignoring the inter-field iteration loop and exchanging the boundary conditions only once every time step.

In CFX, the deformation of boundaries can be taken into account using the ALE formulation [18]. With the additional possibility to exchange boundary conditions at certain points in the solution algorithm, a simple explicit coupling scheme can be realized.

Realizing implicit coupling within the given solution algorithm is more sophisticated and non-trivial. In most implicit solution schemes, it is the case that if there is no convergence within the coupled solution after one inter-field iteration, the solution in the fluid field is reset to the one at the end of the previous time step and the time step is repeated with updated boundary conditions received from the structural code. Therefore, the fluid simulation code has to support 'time staggering.'

Here, a different implementation of the implicit coupling scheme was chosen (Figure 5). The basic idea is that the solution algorithm should be modified as little as possible by the additional functionalities required to perform an implicit-coupled FSI analysis. This is realized by modifying

DOI: 10.1002/fld

the coefficient iteration loop: until the solution within the coefficient iteration loop is converged, the solution algorithm remains unchanged. Once the convergence criterion for the solution of the coefficient loop iteration is satisfied, the computed interface loads are sent to the structural code. Additionally, the simulation code receives notification, if the convergence for the coupled solution is reached. If not, the CFD mesh is updated with the new interface geometry and the computation continues within the coefficient iteration loop. Once convergence for the coupled solution is reached, the simulation code proceeds in time.

The state of convergence of the coupled computation for one time step is judged upon the interface geometry change since the last inter-field iteration step. This convergence check for the coupled solution is done in the structural code. On the fluid side, the convergence status has only to be received.

The advantage of this approach is that the complete FSI inter-field iteration loop is implemented within the structure of the coefficient loop. Considering all additional FSI-specific steps of the inter-field iteration loop as functions which can be skipped, if the convergence criterion within the coefficient loop is not fulfiled, the coefficient loop and the inter-field iteration loop are identical. Therefore, the solution algorithm of the fluid solver 'does not know or need to know' of the existence of an additional inter-field iteration loop. From the point of view of the solver, only additional cycles in the coefficient iteration loop are performed. This extension of the solution scheme is applicable for FSI implementations in CFD codes, which do not support 'time step repetition.'

5. NUMERICAL EXAMPLES

5.1. Hanging roof

The following example presents a hanging membrane roof under wind loading. The set-up is 3D. For the sake of computational efficiency, the depth of the channel is limited and appropriate fluid boundary conditions are applied to reduce the problem to quasi-2D.

The parabolic inflow velocity profile has a maximum velocity of 26 m/s. Figure 6 shows the simulation set-up and a detail of the roof including the CFD grid: the structure consists of a membrane roof with a span of 10 m pre-stressed by its own weight and bordered by rigid walls. The membrane material is a polyester fabric with PVC coating of type I and a thickness of 1 mm. The structural analysis is performed with four-node membrane elements using the generalized-α method to solve the dynamic problem. In the fluid analysis, a SST-turbulence model with wall functions is applied and the fluid properties are those of air at 25°C.

With this set-up, the simulation comprises interaction between incompressible fluid and flexible, extremely light structure. As explained in Section 4, for the analysis by partitioned methods this set-up formulates a sophisticated problem. In order to solve it, the choice of an appropriate coupling scheme and parameters have to be analysed.

Applying explicit coupling results in unstable behaviour for all selected time step sizes in the range from 0.01 to 0.1 s. As the time step is decreased, the instabilities occur sooner.

For implicit, iterative coupling schemes, a time step size of 0.1 s proved to be a good compromise between a sufficient time resolution and a reasonable computational effort. Hence, it will be used in the following computations. The under-relaxation technique presented in Chapter 4 is used

DOI: 10.1002/fld

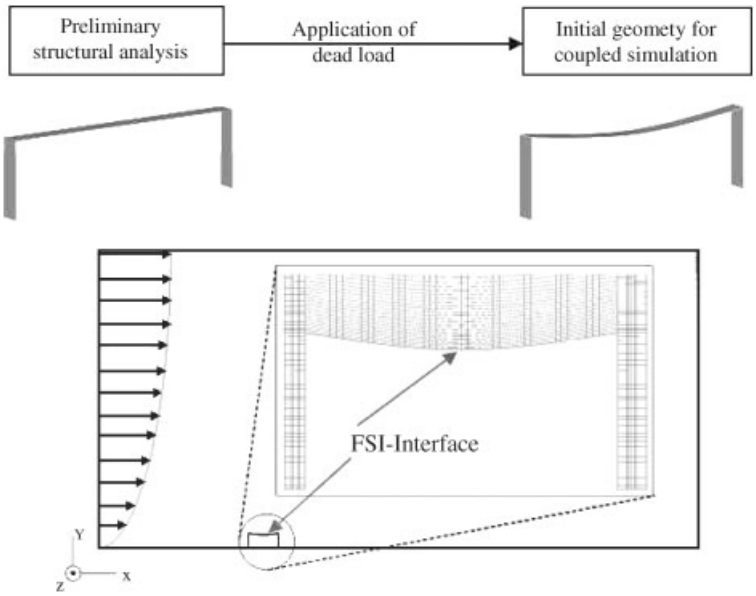

Figure 6. Set-up for the simulation of a hanging roof under wind loading.

for stabilization of the coupled solution. It is applied to the transferred loads or the transferred displacements. Without stabilization (under-relaxation factor $r_{\text{const}} = 1.0$), the implicitly coupled analysis shows no convergence within a time step. As the under-relaxation factor is lowered, the stability of the coupled computation improves. Under-relaxation of displacements appears to be more effective than that of loads.

The upper part of Figure 7 provides a comparison for selected calculations with implicit coupling schemes using fixed under-relaxation factors or adaptive under-relaxation by Aitken's Method. The lower part of Figure 7 shows the time—'number of inter-field iterations'—curve for adaptive Aitken stabilization. Especially in the zoomed view, iterations of the coupling algorithms are visible, as the solution converges towards equilibrium within each time step. Once a stable simulation behaviour is achieved, the stabilization technique itself has little influence on the results.

However, stability has to be paid for by computational effort. Considering the accumulated number of inter-field iterations gives an approximation of the computational effort for different under-relaxation factors in implicit partitioned computations. On this basis, Table I gives a comparison of the relative computational efforts for different under-relaxation factors. With respect to the relative effort, the superiority of the adaptive stabilization is obvious.

Concerning the mechanics of the problem, the simulation gives the expected upward movement, 'snap-through,' and following oscillation of the membrane roof. Figure 8 shows deformation and flow around the roof after the 'snap-through.'

5.2. 3D four-point tent structure subjected to wind

The experiences of the preceding example shall now be extended to a more complex geometry under simplified wind loading. The inflow profile is logarithmic according to the requirements of

DOI: 10.1002/fld

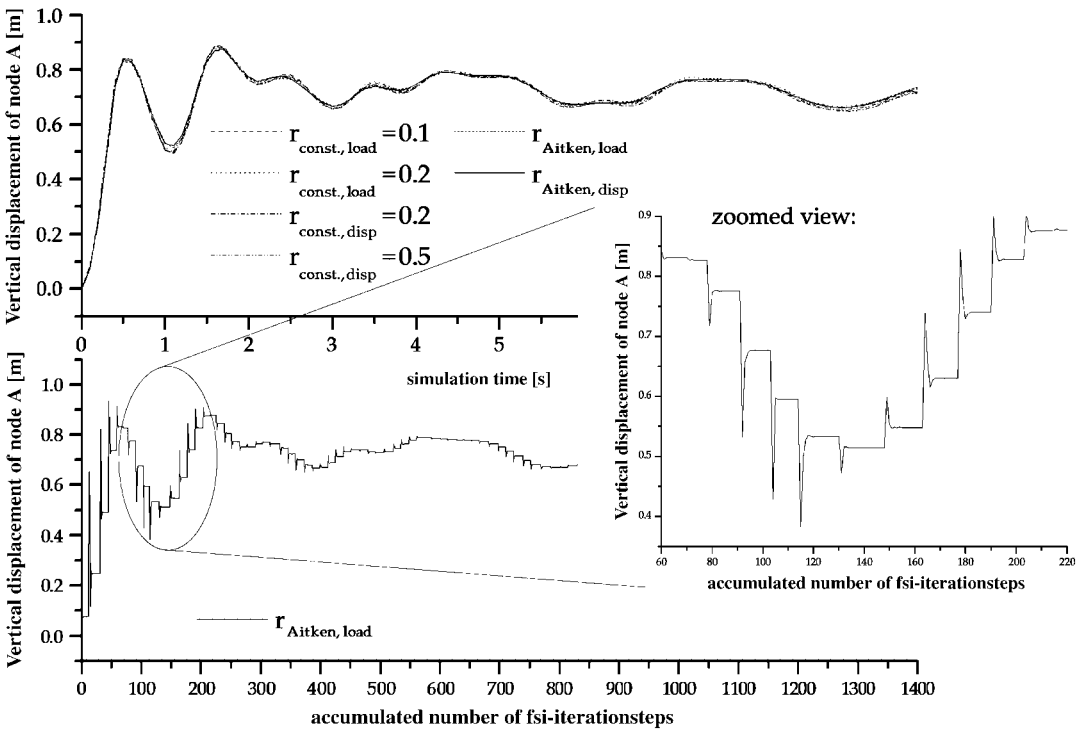

Figure 7. Implicit-coupling procedures using under-relaxation for stabilization: iterations and results.

Table I. Numerical effort for different under-relaxation factors.

Under-relaxation factor	Relative numerical effort (%)
$r_{\text{const., load}} = 0.1$	100
$r_{\text{const., load}} = 0.2$	62
$r_{\text{const., disp}} = 0.2$	64
$r_{\text{const., disp}} = 0.5$	36
$r_{\text{Aitken, load}}$	28
$r_{\text{Aitken, disp}}$	27

German building code DIN 1055-2. The four-point tent structure resembles a saddle surface of a membrane with a uniform pre-stress of 2.5 kN/m stabilized by four cables at the edges pre-stressed with 50 kN. It is supported by two masts constructed from steel tubes with a diameter of 88.9 mm and a thickness of 6 mm. The bracing consists of two sets of two guy cables with a diameter of 13.8 mm, pre-stressed with a force of 41 kN. The membrane material is a polyester fabric with PVC coating of type I and a thickness of 1 mm. The edge cables are spiral strands with a diameter of 16 mm. Dimensions are given in Figure 9.

The set-up of the analysis follows the flow chart given in Figure 1, including the form finding procedure to acquire the proper equilibrium configuration, which defines the initial geometry for the

DOI: 10.1002/fld

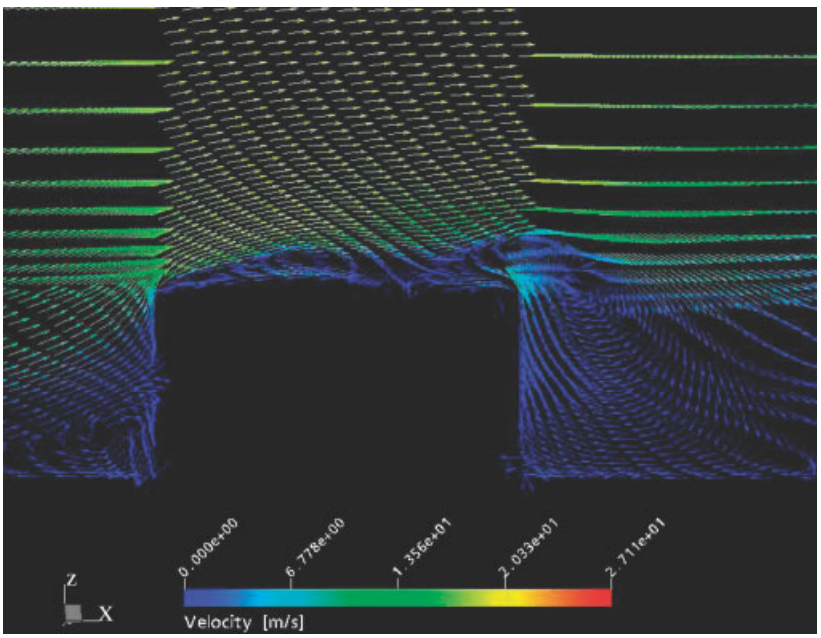

Figure 8. Deformation of membrane roof and velocity vectors.

multiphysics computation. In the fluid domain only the membrane itself is modelled, the influence of cables and masts on the flow field are neglected. For the form finding and the structural analysis, masts and cables are fully taken into account. The interface is treated as a two-sided infinitely thin surface in both the structure and the flow analysis.

The simulation set-up is completely 3D using a tetrahedral mesh for the CFX simulation with refinement by prism layers nearby the membrane and the bottom. A SST-turbulence model with appropriate wall functions is applied. In the structural analysis, three-node membrane elements are used for nonlinear analysis. The fluid is air at 25°C.

The dynamic behaviour of the coupled system was analysed in a transient FSI simulation for a flow in y-direction (Figure 10).With regard to the low structural mass and the incompressible fluid modelling, which in turn is due to the low flow speed of wind, the coupled computation was carried out in a fully implicit manner. The need for this stabilization in the partitioned solution of FSI between light-weight structures and incompressible fluid flows was already described in Section 4 and demonstrated in Section 5.1. To enhance the convergence behaviour in the inter-field coupling loops, Aitken's method was applied. The time integration used on the fluid side was a second-order backward-Euler scheme. On the structural side, the generalized-α method was applied.

The fluid simulation was started from the result of a steady-state solution of flow around the undeformed membrane at 20 m/s. Therefore, the unloaded and undeformed membrane first needs to find its equilibrium state for this inflow velocity. As a result of the stationary computation, an upward deformation occurs in the front part, while the rear part deforms downwards.

DOI: 10.1002/fld

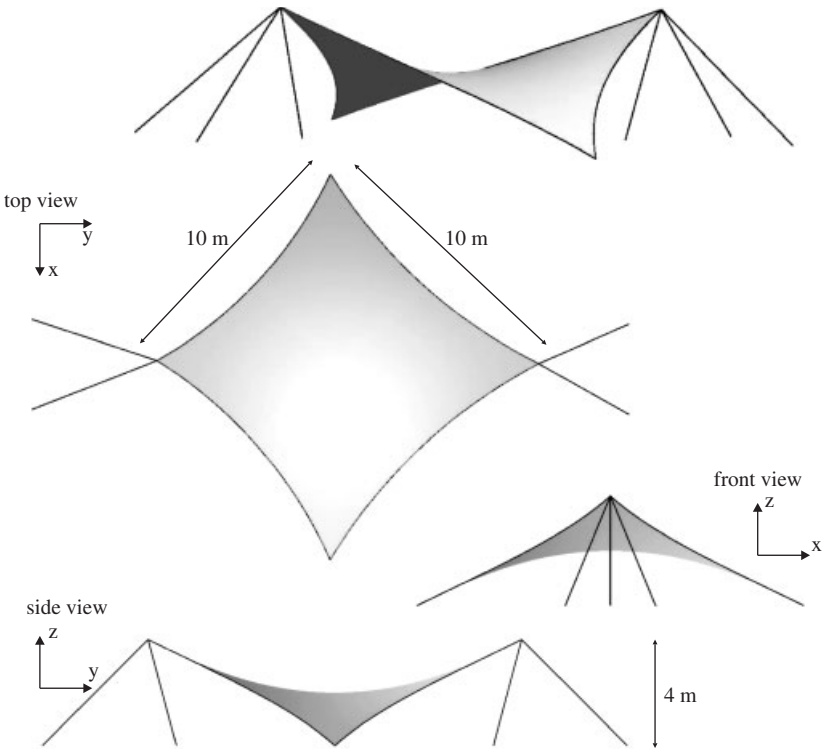

Figure 9. Geometry and dimension of the four-point tent structure.

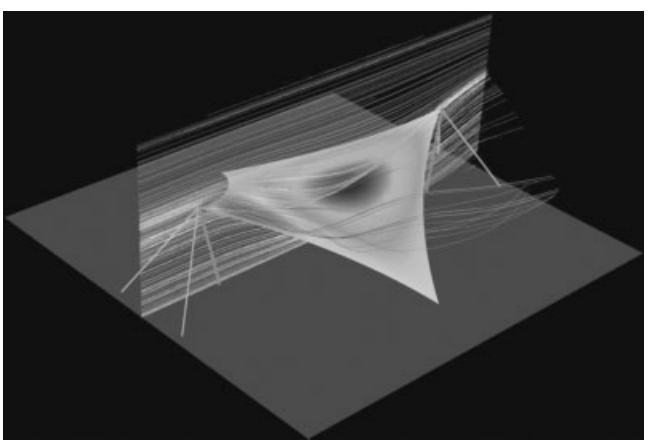

Figure 10. Flow around the membrane.

In the following, the maximum wind speed was varied between 10 and 30 m/s in a gust-like behavior. Figure 11 shows the maximum inflow velocity. The resulting membrane motion is depicted in Figure 12 for different time steps. The structural deformation follows the

DOI: 10.1002/fld

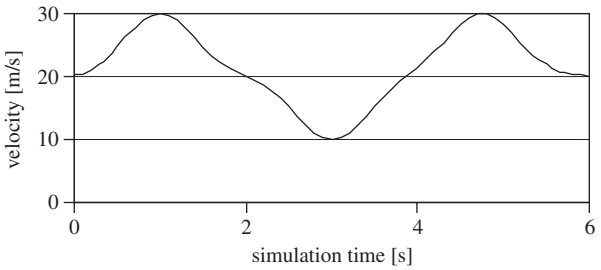

Figure 11. Inflow velocity over simulation time.

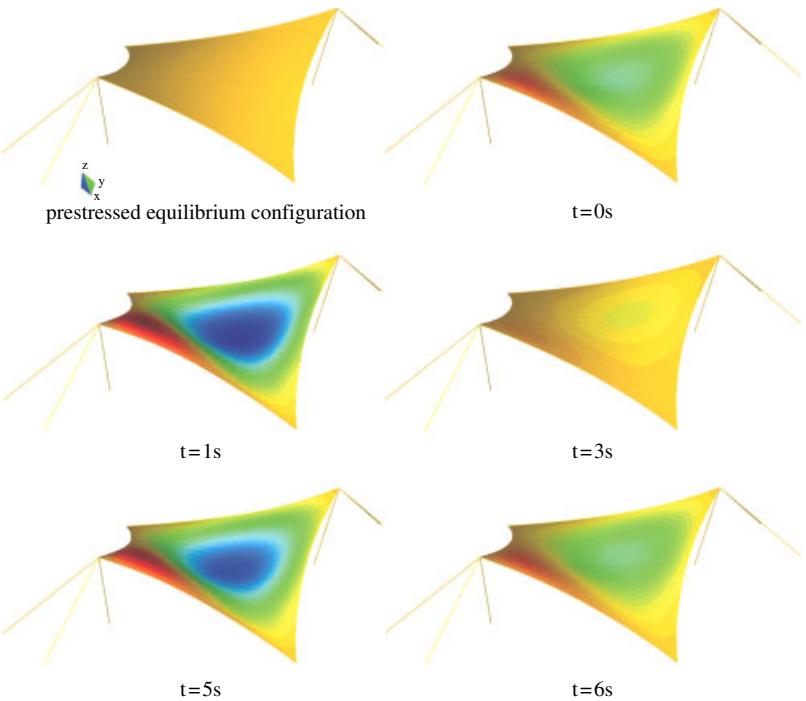

Figure 12. Deformation of four-point tent at different times.

variation of the wind speed without delay due to the membrane's pre-stress and its small mass, which indicates the small influence of the mass of the membrane on the inertia of the complete system.

These results provide a first assessment of the structure's behaviour under wind loading, both in magnitude of the deformation and in the occurring frequencies. Thereby, a possibility arises to quantify the effects, which are expected due to the geometry and the problem setting.

DOI: 10.1002/fld

6. CONCLUSION

In this paper, a modular software environment using the methods of FSI for the simulation of wind effects on light-weight structures, like tents or membrane roofs, was presented.

To take into account all demands arising from the physical problem, a partitioned approach using highly developed codes for the single-field computations, namely CARAT and CFX-5, is applied.

Strongly and weakly coupled iteration schemes were described. It is pointed out that in the case of flexible, nearly mass-less structures interacting with incompressible fluids, implicit coupling schemes are necessary. For the stabilization of implicit coupling schemes, an adaptive under-relaxation technique is applied. This coupling algorithm is realized within the chosen software environment, tailored to the specific needs of the considered problem. Special emphasis was put on the realization of an implicit coupling scheme using the commercial software package CFX-5.

The application of the proposed software environment and the frame algorithm is presented in two examples. The first example concentrates on a quasi-2D transient numerical experiment: a hanging roof structure subjected to wind flow. Detailed analyses with respect to different coupling schemes were performed. It showed necessity for and effects of stabilization. Using the data from the first example, a problem of engineering interest was computed: the stabilized coupling approach was extended to a transient analysis of a wind loaded tent structure, of which the geometrical definition was derived by the stabilized form finding procedure (URS).

Considering the requirements towards the occurring turbulence and the boundary conditions, it is obvious that further improvements are necessary in order to precisely approach the effects of wind loads. However, these first results provide experiences about the difficulties of coupled computations in the field of wind engineering and ideas how to overcome them.

ACKNOWLEDGEMENTS

The authors gratefully acknowledge the support of Dr.-Ing. Martin Kuntz from ANSYS Germany GmbH for ongoing interest to establish a coupled computation using CFX-5.

REFERENCES

1. Bletzinger K-U, Wüchner R, Daoud F, Camprubí N. Computational methods for form finding and optimization of shells and membranes. *Computer Methods in Applied Mechanics and Engineering* 2005; **194**:3438–3452.
2. Forster B, Mollaert M. *European Design Guide for Tensile Surface Structures*, TensiNet, 2004.
3. Farhat C. CFD-based nonlinear computational aeroelasticity. In *Encyclopedia of Computational Mechanics*, Stein E, de Borst R, Hughes TJR (eds). Wiley: Chichester, 2004; 459–480.
4. Bazilevs Y, Calo VM, Zhang Y, Hughes TJR. Isogeometric fluid–structure interaction analysis with applications to arterial blood flow. *Computational Mechanics* 2006; **38**:310–322.
5. Michler C, van Brummelen EH, de Borst R. An interface Newton–Krylow solver for fluid–structure interaction. *International Journal for Numerical Methods in Fluids* 2005; **47**:1189–1195.
6. Sawada T, Hisada T. Fluid–structure interaction analysis of the two dimensional flag-in-wind problem by an interface tracking ALE finite element method. *Computers and Fluids* 2007; **36**:136–146.
7. Tezduyar TE, Sathe S, Keedy R, Stein K. Space–time finite element techniques for computation of fluid–structure interactions. *Computer Methods in Applied Mechanics and Engineering* 2006; **195**:2002–2027.
8. Tezduyar TE, Sathe S, Stein K. Solution techniques for the fully-discretized equations in computation of fluid–structure interactions with space–time formulations. *Computer Methods in Applied Mechanics and Engineering* 2006; **195**:5743–5753.

DOI: 10.1002/fld

9. Cebral JR. Loose coupling algorithms for fluid–structure interaction. *Dissertation*, George Mason University, 1996.
10. Farhat C, Lesoinne M. Two efficient staggered algorithms for the serial and parallel soluation of three-dimensional nonlinear transient aeroelastic problems. *Computer Methods in Applied Mechanics and Engineering* 2000; **182**: 499–515.
11. Glück M. Ein Beitrag zur numerischen Simulation von Fluid–Struktur-Interaktionen—Grundlagenuntersuchungen und Anwendung auf Membrantragwerke. *Dissertation*, Universität Erlangen, 2002.
12. Kalro V, Tezduyar TE. A parallel 3D computational method for fluid–structure interactions in parachute systems. *Computer Methods in Applied Mechanics and Engineering* 2000; **190**:321–332.
13. Stein KR, Benney RJ, Tezduyar TE, Leonard JW, Accorsi ML. Fluid–structure interactions of a round parachute: modeling and simulation techniques. *Journal of Aircraft* 2001; **38**:800–808.
14. Felippa CA, Park KC, Farhat C. Partitioned analysis of coupled mechanical systems. *Computer Methods in Applied Mechanics and Engineering* 2001; **190**:3247–3270.
15. Le Tallec P, Mouro J. Fluid structure interaction with large structural displacements. *Computer Methods in Applied Mechanics and Engineering* 2001; **190**:3039–3067.
16. Mittal S, Tezduyar TE. Parallel finite element simulation of 3D incompressible flows—Fluid–structure interactions. *International Journal for Numerical Methods in Fluids* 1995; **21**:933–953.
17. Stein K, Benney R, Kalro V, Tezduyar TE, Leonard J, Accorsi M. Parachute fluid–structure interactions: 3D-computation. *Computer Methods in Applied Mechanics and Engineering* 2000; **190**:373–386.
18. CFX ANSYS Inc. *CFX-5.7 Documentation*, 2004.
19. Fraunhofer Institute for Algorithms and Scientific Computing. *MpCCI specification*, *version 2.0*, 2003.
20. Ferziger JH, Perić M. *Computational Methods for Fluid Dynamics* (2nd edn). Springer: Berlin, 1999.
21. Menter FR. Two-equation eddy-viscosity turbulence models for engineering applications. *AIAA Journal* 1994; **32**(8):1598–1605.
22. Kuntz M, Menter FR. Numerical flow simulation with moving grids. *STAB Conference*, Bremen, 2004.
23. Johnson AA, Tezduyar TE. Mesh update strategies in parallel finite element computations of flow problems with moving boundaries and interfaces. *Computer Methods in Applied Mechanics and Engineering* 1994; **119**:73–94.
24. Stein K, Tezduyar T, Benney R. Mesh moving techniques for fluid–structure interactions with large displacements. *Journal of Applied Mechanics* 2003; **70**:58–63.
25. Chung J, Hulbert GM. A time integration algorithm for structural dynamics with improved numerical dissipation: the generalized-α method. *Journal of Applied Mechanics* 1993; **60**:371–375.
26. Schweizerhof K, Ramm E. Displacement dependent pressure loads in nonlinear finite element analyses. *Computers and Structures* 1984; **18**(6):1099–1114.
27. Wüchner R, Bletzinger KU. Stress-adapted numerical form finding of pre-stressed surfaces by the updated reference strategy. *International Journal for Numerical Methods in Engineering* 2005; **64**:143–166.
28. Bletzinger K-U, Ramm E. A general finite element approach to the form finding of tensile structures by the updated reference strategy. *International Journal of Space Structures* 1999; **14**(2):131–145.
29. Piperno S. Explicit/implicit fluid/structure staggered procedures with a structural predictor and fluid subcycling for 2D inviscid aeroelastic simulations. *International Journal for Numerical Methods in Fluids* 1997; **25**:1207–1226.
30. Piperno S, Farhat C. Partitioned procedures for the transient solution of coupled aeroelastic problems. Part II: energy transfer analysis and three-dimensional applications. *Computer Methods in Applied Mechanics and Engineering* 2001; **190**:3147–4170.
31. Mok DP. Partitionierte Lösungsansätze in der Strukturdynamik und der Fluid–Struktur-Interaktion. *Dissertation*, Universität Stuttgart, 2001.
32. Mok DP, Wall WA. Partitioned analysis schemes for the transient interaction of incompressible flows and nonlinear flexible structures. In *Trends in Computational Structural Mechanics*, Wall WA, Bletzinger KU, Schweizerhof K (eds). CIMNE: Barcelona, 2001; 689–698.
33. Causin P, Gerbeau JF, Nobile F. Added-mass effect in the design of partitioned algorithms for fluid–structure problems. *Computer Methods in Applied Mechanics and Engineering* 2005; **194**:4506–4527.
34. Wall WA. Fluid–Struktur-Interaktion mit stabilisierten Finiten Elementen. *Dissertation*, Universität Stuttgart, 1999.
35. Foerster C, Wall WA, Ramm E. Artificial added mass instabilities in sequential staggered coupling of nonlinear structures and incompressible viscous flows. *Computer Methods in Applied Mechanics and Engineering* 2007; **196**:1278–1293.
36. Turek S, Hron J. Proposal for numerical benchmarking fluid–structure interaction between an elastic object and laminar incompressible flow. In *Fluid–Structure Interaction—Modelling*, *Simulation*, *Optimisation*, Bungartz H-J, Schäfer M (eds). Lecture Notes in Computational Science and Engineering, vol. 53. Springer: Berlin, 2006.

DOI: 10.1002/fld

37. Irons BM, Tuck RC. A version of the Aitken accelerator for computer iteration. *International Journal for Numerical Methods in Engineering* 1969; **1**:275–277.
38. Bletzinger K-U, Wüchner R, Kupzok A. Algorithmic treatment of shells and free form-membranes in FSI. In *Fluid–Structure Interaction—Modelling*, *Simulation*, *Optimisation*, Bungartz H-J, Schäfer M (eds). Lecture Notes in Computational Science and Engineering, vol. 53. Springer: Berlin, 2006.

DOI: 10.1002/fld